Paper 67

The Creation of a Gas-Liquid Nozzle with Predictable Behaviour

A.V. Karpyshev, A.V. Tsipenko and A.A. Yakovlev
Scientific Research Center of Advanced Technologies
Moscow State Aviation Institute - MAI, Moscow, Russia

Abstract

The Euler-Euler models of different complexity levels (from one-dimensional monodisperse model to two-dimensional polydisperse model with drop interaction one) are used for acceleration nozzle design.

The optimum value of liquid-to-gas mass flow rate ratio was defined theoretically and experimentally in maximum range nozzle-jet system.

The numerical-and-experimental method of searching optimal condition for "mixer+nozzle" system has been formulated. A method of mixture generation has been selected.

The experimental investigations of adjusted nozzles were made in order to define a physical flow model and to estimate the application of mathematical models. Photo- shooting in the flash light (duration from 10^{-6} s) was used. Gas and liquid mass flow rate, distribution of pressure along a convergent-divergent nozzle wall were measured. Modified probe and laser methods were used in order to receive gas and liquid velocity and volume concentration data.

It is shown that the flow structure in or near the nozzle is fragmentary (cluster), in other words the flow contains not only drops, but also fragments of liquid film. For such flows the numerical models are used as minimax estimate. The outcomes of numerical simulation are presented in this paper too.

Keywords: gas-liquid flow, convergent-divergent nozzle, Euler-Euler model, experimental investigations.

1 Introduction

Water mist application dramatically increases fire-fighting efficiency. Fire statistics and test data analysis performed by Research Institute of Ministry of Emergency Situations of Russia has shown that while extinguishing most common fires a liquid flow rate should be about 0.5 L/s, water droplet size at the fire site - ~150 mcm, with

operator's distance away from the fire – up to 5 in. The easiest way to deliver the atomized liquid is to supply it in the form of a jet, herewith efficient atomization may be achieved with gas-liquid nozzle application, when the liquid is broken into tiny droplets and accelerated in a gas flow. A method of designing these nozzles and nozzle flow description are given below. Present results were used to creation of gas-liquid jet fire-fighting systems (from backpack to helicopter-based ones).

2   Basic flow parameter determination

First of all, it is important to know discrete phase parameters which determine a gas-drop jet compactness.

As a criterion of compactness the appointed minimum value of a volume concentration of particles (drops) will be used hereinafter, which corresponds to "transparency", "visibility" or "optical thickness" concepts of a two-phase jet and allows to compare numerical and experimental data directly by the results of photography and videofilming.

For practical objects it is necessary to know how to forecast compactness of a jet depending on nozzle exit section parameters of the flow, and it is desirable to have criteria relations, i.e. the relations to the dimensionless characteristics of a flow. Some basic flow performance parameters are Reynolds number of a gas phase Re_g, slip of Up/Ug discrete phase (particle velocity Up to gas velocity Ug ratio), mass concentration of particles in the Gp/Gg flow (particle flow rate Gp to gas flow rate Gg ratio), volumetric concentration of particles in the flow Ap, relative size (diameter) of particles Dp/d (d- outlet nozzle diameter, Dp – particle diameter).

The influence of these criteria on compactness of monodisperse heterogeneous jet was numerically investigated with the use of original [1,2] and the determining (basic) criteria were excreted.

Ap examination for different Up/Ug values shows that it has no direct dependence on Re_g. That could be explained by surrounding air entrail, gas impulse decrease, and decrease of transversal turbulence diffusion of particle, accordingly. And the less "energetic" jet can be more compact. The Up/Ug influence is sufficiently weak in the area at a certain distance from the jet. But Gp/Gg influence on jet compactness is stronger.

There is strong relation to Dp, and jet compactness is proportional to Dp. But Dp is determined.

The computation run for air- water jet was performed under the following conditions: nozzle inlet static air pressure had to be unchanged and equal to 5 atm, $Up=Ug \approx 5$ m/s, inlet nozzle diameter had to constant. Nozzle parameters were selected to maximize Up and minimize $|Up-Ug|$, and nozzle outlet static air pressure is equal to static pressure of the ambient air. If first to blow the air through the nozzle and then add more and more water drops, there'll be a hose barrel jet as a result. Average velocity of such gas-drop mixture decreases steadily, but jet range is non-linear in relation to Gp/Gg.

In Figure 1 jet centerline parameter variation (Ap, Up) and jet width as Gp/Gg function were shown, R- distance from the jet axis. There is a strong relation to Gp/Gg, and when $Gp/Gg=30$ Ap slightly decreases along a jet centerline, i.e. this jet

is long and compact. There is strong relation to Ap, but Gp/Gg is proportional to Ap. So it makes no sense to use Ap as special criterion for jet compactness estimation.
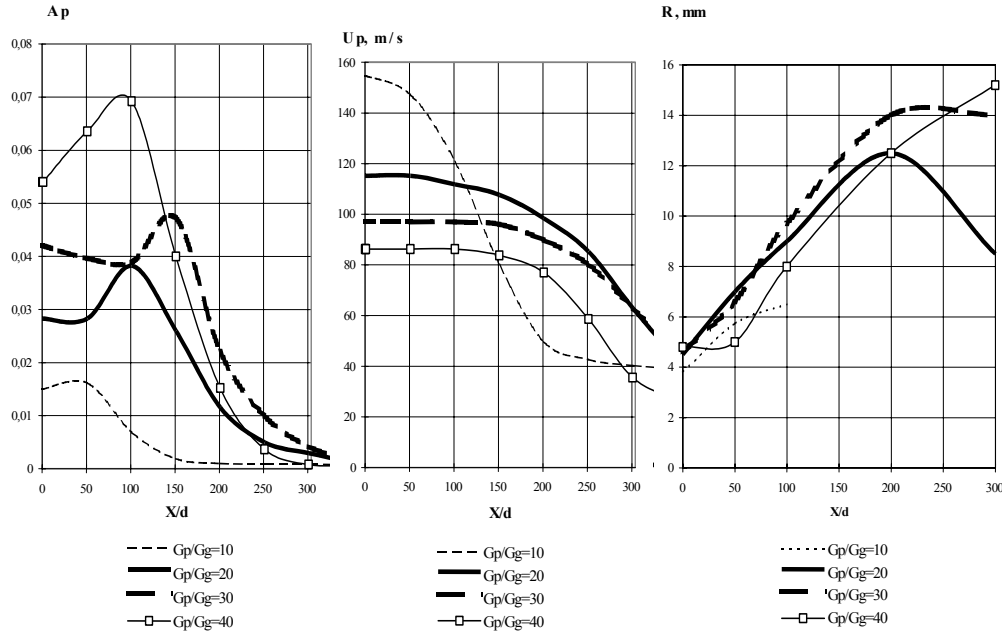

Figure 1: Variation of jet centerline parameters (Ap,Up) and jet width as Gp/Gg function.

On the basis of the outcome calculation analysis it is possible to make the following conclusion: there is such Gp/Gg ratio when gas-drop range is greater than the hose barrel jet range with equal inlet pressure, and we can assess Gp/Gg optimal quantity.

Voronetsky [3] conducted the experiments to investigate gas-water jet range. The experimental configuration consisted of air and water lines combining chamber, separable nozzles (outlet diameters 7 to 11 mm), monitoring and control devices. Gp/Gg changed up to 64, inlet static air pressure was between the limits of 4.5 and 5.5 atm. In Figure 2 a maximum distance, when Gp/Gg is within the range of 30-40, is shown.

To determine parameters at the initial jet cross-section, at the nozzle exit, a monodimensional and monodisperse model of nozzle section design by a pre-set pressure difference was used. The same model is used to obtain the first nozzle section version. Hereto a nozzle section accepted for manufacture is slightly different from that one. This is explained by taking into account the mixing chamber structure features, calculation results with axisymmetric monodisperse Euler-Euler model ignoring interaction between droplets [4] and manufacturing limitations. Fig. 3 shows a nozzle section calculated by monodimensional model (R_{nozzle}) and a manufactured one (R_{real}).
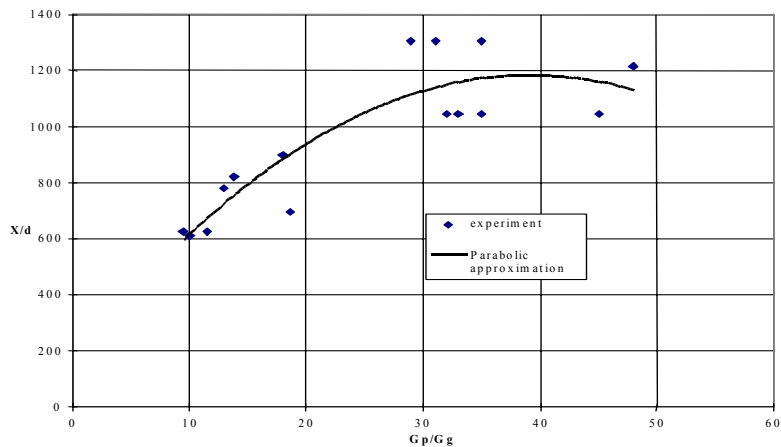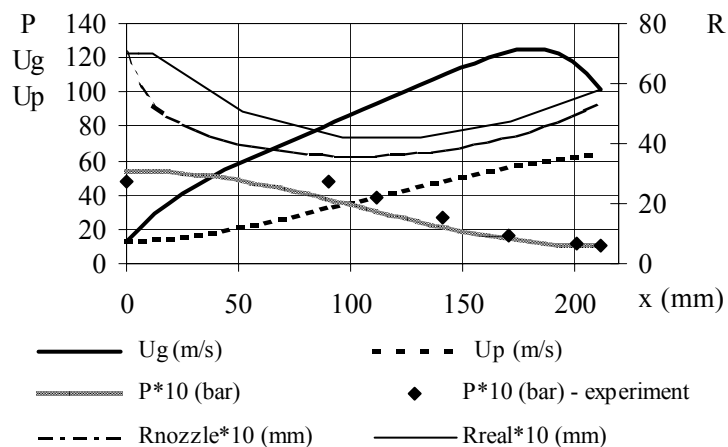
3

Figure 2: Experimental jet range results.

Figure 3: Nozzle section calculated by monodimensional model (R_{nozzle}) and a manufactured one (R_{real}), P-gas pressure, X-distance along the nozzle.

3 Design- and- test techniques of nozzle gas-and-liquid mixture efficiency

As liquid share is considerably great, you never know the nozzle flow structure. It is difficult to know the nozzle flow structure. It is difficult to determine liquid film parameters on the wall, gaseous and liquid phase condition (dispersed composition of inclusions, temperature, velocity and other parameters across the nozzle, particularly, at the nozzle exit cross-section).

Due to a difficulty to simulate gas-and-liquid–mixing processes constructive decisions are made mostly after the tests. With this approach it is very difficult to find out the reason when a system fails to give a design jet. It is a dilemma to guess

4

either a "bad" nozzle would not accelerate a "good " flow of droplets or it is the other way round or the operating mode is wrong. Therefore, an optimum operating mode is urgent for a particular design and it should be done with the least costs. A possible way to solve this problem is given below.

An ideal flow (in the meaning of energy transfer from gas to droplets) may be the so-called "equilibrium" flow, in which the droplets instantly accept gas velocity. This flow parameters are determined by a well-known technique [5]. Gas flow rate dependence on liquid on liquid flow rate may be determined experimentally. The same dependence may be hypothetically determined for "equilibrium" mixture. Figure 4 demonstrates flat nozzle flow rate data in comparison between the test items [6] and those obtained by "equilibrium" model. Figure 5 compares similar flow rate data of a testing axisymmetric nozzle.
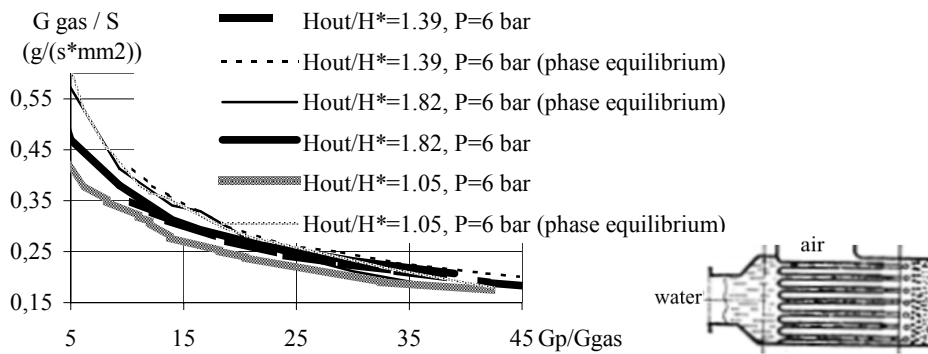

Figure 4: Mixing chamber diagram, an experimental one and that obtained under phase equilibrium representing nozzle flow rate data [6]. Air flow rate [g/(s·cm^2)] per nozzle throat area unit in relation to system water mass concentration.
P – nozzle inlet pressure, H* - nozzle throat height,
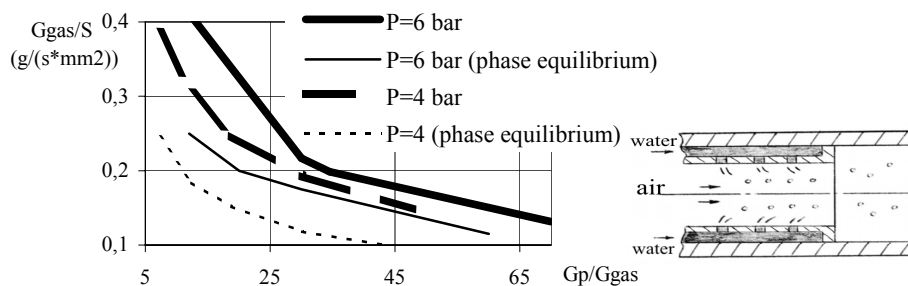H_{out} – nozzle exit section height.

Figure 5: Mixing chamber diagram, an experimental one and that obtained under phase equilibrium representing nozzle flow rate data.

The analysis of different-configuration nozzle operation and different gas-and-liquid –mixing processes ahead of the nozzle [7] shows that a test and hypothetic

phase flow rate interposition characterizes a transverse liquid distribution, namely: with a hypothetic curve located higher in the graph an experimental flow is sufficiently homogeneous, the dependence difference caused by phase velocity difference; with a contrary disposition the difference is caused by the fact that there is a lot of film and quite a solid liquid nucleus (stream) inside the nozzle or, which is the same, there are areas with little liquid mass compared with the core.

A supposition set forward allows to select an operating mode and system improvement direction quite easily. An optimum mode is in the vicinity of hypothetic and experimental curve intersection point. With a hypothetic curve position higher than that of an experimental one the main efforts have to be aimed at passage section design, otherwise a mixing chamber has to be updated.

A water supply method, as the simplest one, for the systems designed is shown in Figure 5. For adjusting a system developed a test series was conducted. The table 1 and Figure 6 give the integral data for an optimum mode (from the viewpoint of range, dispersion and compactness). They are slightly different from the design ones, which confirms applicability of a method accepted. Figure 7 demonstrates a test system gas-droplet jet range.

Basic outlet diameter	11.6 mm
Mean gas velocity	90 m/s
Mean droplet velocity	56 m/s
Gas mass flow rate	12.7±0.2 g/s
Droplet mass flow rate	397±4g/s
Nozzle inlet pressure	4.5 atm

Table 1: Basic parameters of an optimum flow in experimental nozzle
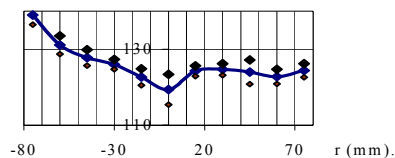

Figure 6: Mean volumetric-surface (Sauter) droplet diameter (mcm) variation along a jet radius at the distance of 2 m from the nozzle exit.

Figure 7: Backpack fire-fighting system jet.

4 Experiments and numerical simulation

To make a physical flow model more definite and receive the data necessary for spatial numerical simulation the local parameters of the nozzle exit section and some nozzle inlet flow data were obtained experimentally.

Nozzle inlet flow photos (a nozzle is on the left, a mixing chamber is on the right) in the flash light 10^{-6}s long are in Figure 8. Figure 8-A represents a photo in "transmitted light" (negative), Figure 8-B – "a light knife" oriented across a passage axis, Figure 8-C – "a light knife " oriented along a passage. One can see there is not any substantial film in the passage. One can estimate the droplet size at the nozzle inlet wall from Figure 8-B. It is ~150 mcm. As the droplets are practically very clear, not blurred, their velocity does not exceed 10 m/s.
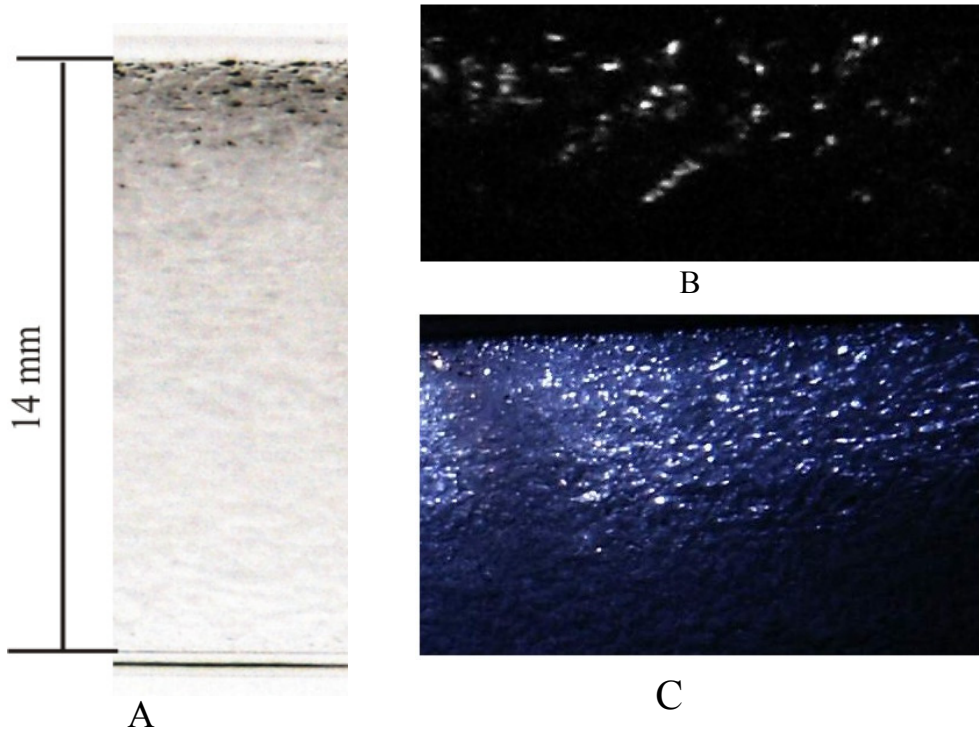

Figure 8: Nozzle inlet flow photos (a nozzle is on the left, a mixing chamber is on the right) in the flash light 10^{-6}s long.

Analyze the photographs taking into account monodimension and monodisperse model calculation results given in Figure 3 (droplet diameter is constant and assumed 140 mcm). The flow parameters are close to experimental ones. With a mean velocity of 13 m/s and 10^{-6} exposure time at the nozzle inlet, i.e. in a cylindrical insert, a droplet displacement will equal to 13 mcm. An average distance between the droplets is 0.93 of their diameter, i.e. the flow has to be transparent, at least at the upper and lower boundaries of the channel. On the other hand, one can see from the photo that inclusions are located at the upper and lower boundaries of

the channel with a greater density than a mean value that may occur either at a velocity higher than the average or at a volumetric concentration of the droplets greater than the average. The latter is most probable. Hence, a maximum of droplet velocity is most likely on the channel axis, a maximum of a volumetric concentration is shifted to the wall, i.e. the flow is of an annular shape. Figure 9 shows possible profiles of gas velocities and Ap volumetric concentration with account of mean velocity values at the nozzle inlet and weak flow transparency directly at the channel walls.
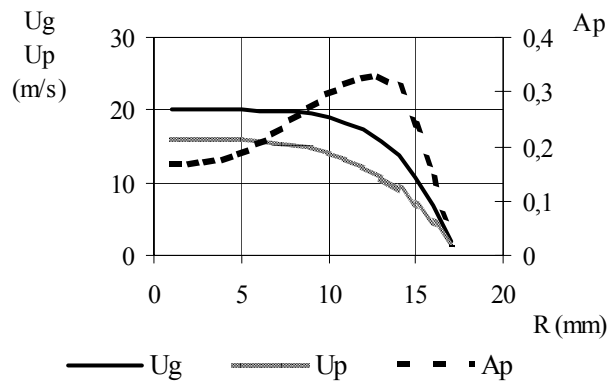

Figure 9: Possible profiles of gas and droplet velocities and Ap volumetric droplet concentration.

Figure 10 shows a jet photo "in the transmitted light " at the nozzle exit section (a nozzle is to the right) in the flash light 10^{-6} s long. One can see a flying liquid film breaking into fragments at the channel outlet flow boundary.
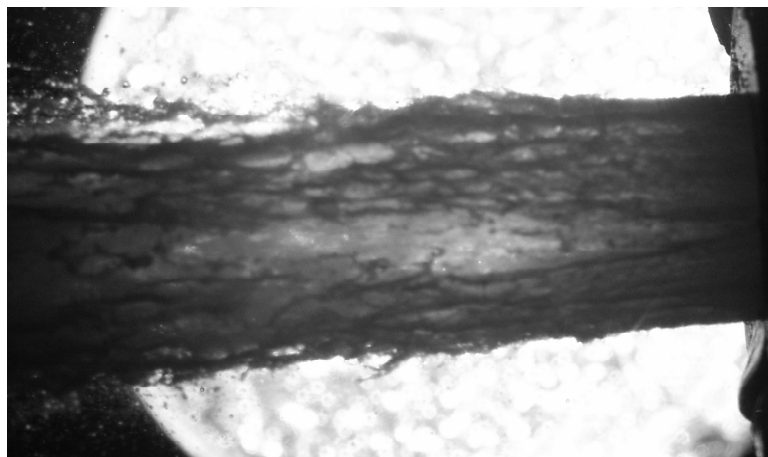

Figure 10: Jet photo in the transmitted light at the nozzle exit (nozzle is on the right) in the 10^{-6} s flash light.

Since the flow is optically dense, a probe-sample selector, a probe – static pressure meter, a probe-meter of a total incoming flow pressure were used to obtain the nozzle exit flow parameters. The measurements were taken at the cross-section 1 (one) diameter distance (11.6 mm) away from the nozzle exit. The probe indications may be interpreted as total pressure of an equilibrium flow but since the air flow rate is considerably less than water flow rate, the following is evident:

$$(P_c+P_{atm}) \cdot S_{probe}+G_p \cdot U_p/2=(P^*+P_{atm}) \cdot S_{probe} \qquad (1),$$

where P_c – static and atmospheric pressure difference measured; S_{probe} – probe area; P^*- total and atmospheric pressure difference measured; P_{atm} – atmospheric pressure. Figure 11 represents the results of probe measurements that confirm a conclusion of an annular flow shape. Therefore a film should be taken into consideration while performing numerical simulation.
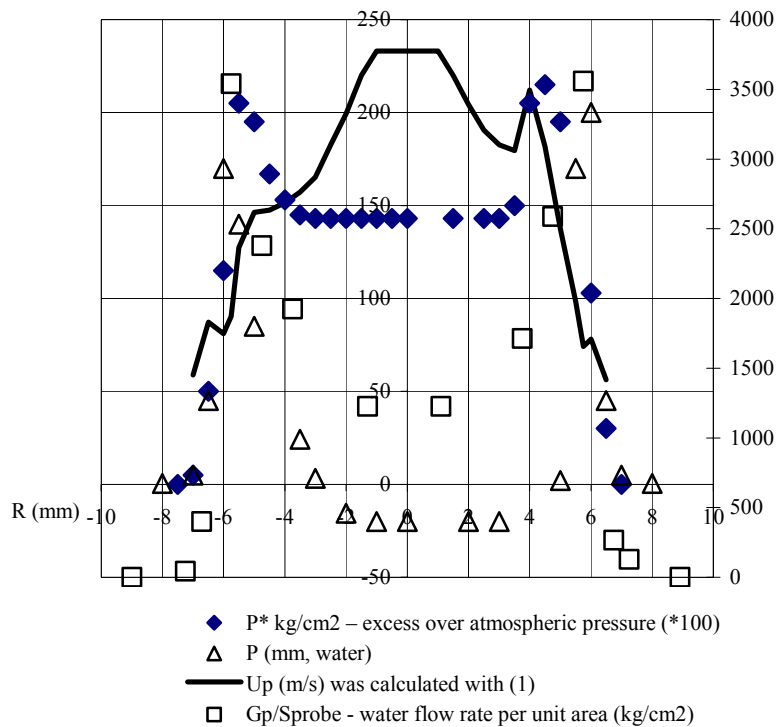

Figure 11: Probe measurement results.

A numerical nozzle flow simulation was performed with experimental data of droplet-to-droplet and droplet-to-film interaction applied [5]. A method of "large particles" [8], which is Harlow's "particles in cells" method development, was also used. Euler-Euler non-stationary models were employed for gas and droplets. A stationary decision was as a limit in solving non-stationary equations. Figure 12 demonstrates the results obtained with application of nozzle inlet parameters from Figure 9. It is seen that there is an area in the diverging part of the nozzle near the wall in the same manner as in the nozzles with a small share of particles [9], where a droplet concentration is lower than the average value along the flow. At first sight it

9

contradicts the probe measurement results. However, an experimental check with application of an electric probe, the diagram of which is given in Figure 13, has shown that a narrow area does exist where liquid is actually absent (area 2 of an abrupt voltage U decrease in Figure 13).
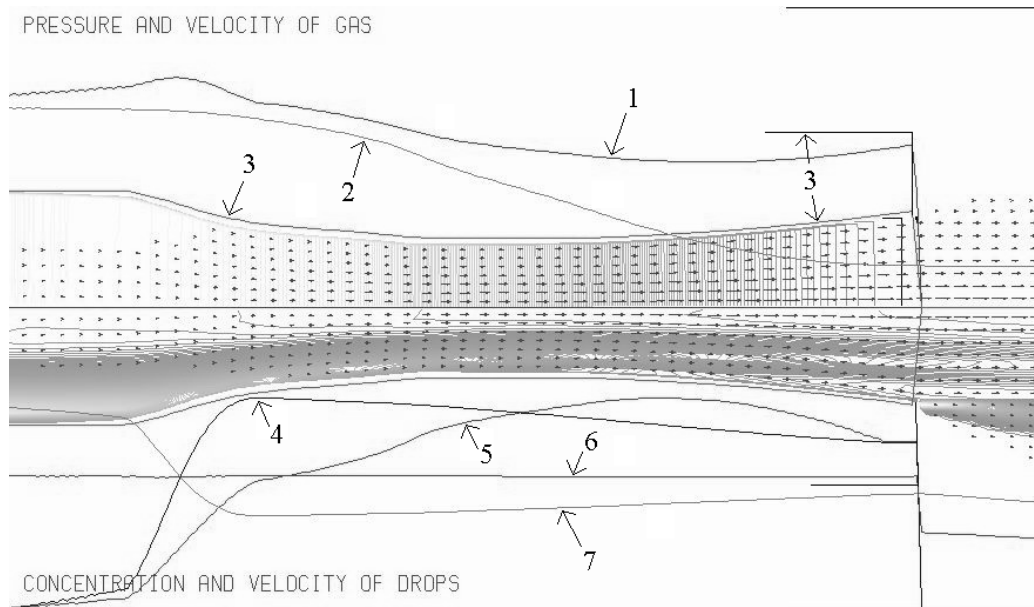

Figure 12: Numerical simulation data visualization. 1 – film boundary (distance from nozzle wall 3, extended scale); 2 – pressure along nozzle wall; 3 – nozzle wall; 4 – film mass flow rate; 5 – film velocity; 6 – total water mass flow rate; 7 – drop mass flow rate.
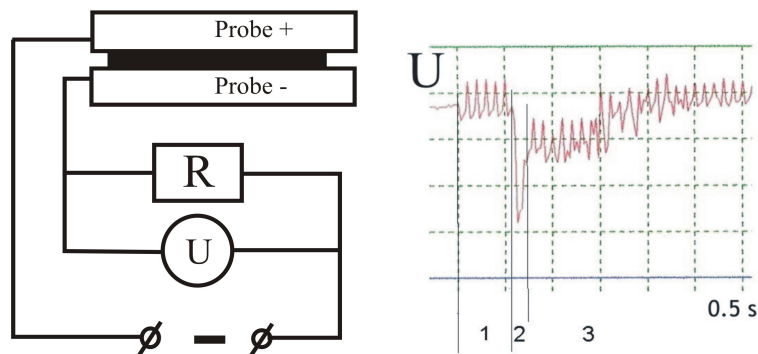

Figure 13: Voltage variation while putting a probe into the flow ~5 mm deep. 1- film signal, 2- small droplet concentration zone signal, 3- flow droplet nucleus signal.

5   Conclusion

The numerical simulation results, the closest to an experiment, have been obtain with wall film friction factor of 0.005 [10], which contributes to a turbulent film flow mode. The gas-film friction factor was also taken from Wallis's work [10]. While employing ratios from papers [11,12] there appeared great film thickness changes. Thus, friction factor agreement is a particularly complex problem.

The test and numerical simulation results confirm design-and-experiment technique substantiation of estimating gas and liquid mixing efficiency in the nozzle. A zone of small liquid content predicted by the above techniques was found out during the tests. As it is seen from Figure 12, the calculations failed to give a good flow homogeneity at the nozzle exit axis of symmetry as it was in the tests. We suppose that it is connected with the fact that the flow in the nozzle throat is wispy-annular, and the liquid flows not in the shape of droplets but fragments with resistance greater than that of droplets. The same flow behaviour is seen at the nozzle exit section. A model of twin impacts applied in this situation [5] also brings an error into calculations.

You can see from the above that the scope and complexity of a calculation model are greater than the abilities of single-processor computers, when you can have the results showing only tendencies and qualitative picture of the flow. By virtue of the above fact the nozzle development procedures are the following:

- to determine a desired water flow rate, limiting pressure and air flow rate, a dominant water droplet diameter, and a minimum jet range;
- to calculate a tentative nozzle section by monodimension model;
- to perform a numerical simulation of the flow by different-complexity – level two-dimension models, the results of which help assess a gas-droplet jet range, correct a nozzle section, come to conclusion of a flow behaviour and possible effect upon the flow;
- flow rate parameters have to be defined at the test facility for a corrected nozzle section with a mixing chamber; by means of design-and-experiment techniques of estimating gas-and-liquid mixing efficiency and numerical simulation the flow rate and pressure parameters are defined more exactly to achieve a maximum jet range.

Acknowledgement

References

[1]   Yu.V.Zuyev, I.A.Lepeshinsky. Two-Phase Multicomponent Turbulent Jet with Phase Transfers, Proceedings of Russian Academy of Sciences, series Liquid and Gas Mechanics, 1995, No. 5, p. 120-138.

[2] V.V.Kostyuk, I.A.Lepeshinsky, Yu.V.Zuyev, O.K.Ivanov, V.A.Reshetnikov, A.V.Voronetsky, A.V.Tsipenko. Interphase Interaction process Investigation in Multiphase Turbulent Jets, Journal Mathematical Simulation, Vol. 11, No 4, 1999, p. 59-69, Moscow, Nauka.

[3] A.V.Voronetsky. Experimental Investigation of Water Mist Fire Fighting Gas-and-Liquid Jet Range // MGTI GA Proceedings, ser. Aeromechanics and Strength, No. 15, 1999, p. 71-72.

[4] I.A.Lepeshinsky, A.A.Yakovlev, G.V.Molesson, A.V.Voronetsky, V.I.Ones, A.V.Tsipenko. Numerical and Experimental Gas-and-Droplet Flow Investigation in the Nozzle with Great Disperse Phase Concentration // Mathematical Simulation, 2002, Vol. 14, No.7, p. 121-127.

[5] L.E.Sternin, A.A.Shriber. Multiphase Gas Flows with Particles. – M., Mashinostroyeniye, 1994.

[6] V.G.Selivanov, K.I.Soplenko, S.D.Frolov. Gas-and-Liquid Media Flow in Desired Geometry Nozzles.// Powerplant Gas and Thermodynamics Items. Thematic Collection of Scientific Transactions. Iss. 2, Kharkov, 1975, KhAI, p.19-27.

[7] A.V.Karpyshev, A.V.Tsipenko. Helicopter-Based Fire Fighting System Operation Optimization. // Materials of the V-th International Scientific-and-Engineering Coference AVIA-2003, Kiev, NAU, 2003, Vol. 2, p. 24207-24208.

[8] O.M.Belotserkovsky, Yu.M.Davidov. A Method of "Large Particles" for Gas Dynamics. Computation Experiment. - M., 1982.

[9] U.G.Pirumov, G.S.Roslyakov. Gas Dynamics of Nozzles. – M.: Science, 1990.

[10] G.B.Wallis. Annular two-phase flow. J. Basic Engng, 1970.

[11] V.A.Barilovich, Yu.A.Smirnov. Numerical Method for Two-Phase Flow in Calculation Variable Cross-Section Nozzlez. –S.-Petersberg, State Technical University, 1997.

[12] I.A.Lepeshinsky, A.A.Buzov. Calculation of Two-Phase Nozzle Flow with Film.// Powerplant Gas and Thermodynamics Items. Thematic Collection of Scientific Transactions. Iss. 4, Kharkov, 1977, KhAI, p.55-66.